Asia Pac. J. Math. 2023 **10**:49

MATHEMATICAL ANALYSIS OF AN HIV MODEL WITH TWO SATURATED RATES, CTL RESPONSE AND THERAPY

B. LAHMIDANI[1], Y. TABIT[2], O. BAIZ[3,*], D. EL MOUTAWAKIL[4]

[1]Univ Sultan Moulay Slimane, FP of Khouribga, Morocco.

[2]Univ Hassan II, ENCG Casablanca, Morocco

[3]Univ Ibn Zohr, FP of Ouarzazate, Morocco

[4]Univ Sultan Moulay Slimane, FP of Khouribga, Morocco

[*]Corresponding author: othman.baiz@gmail.com

Received Oct. 3, 2023

Abstract. The purpose of this paper is to introduce and investigate a new dynamic system that describes the infection of the human immunodeficiency virus (HIV) involving cytotoxic T-lymphocytes (CTL), while also exploring and studying two saturated rates. The model incorporates two treatments that represent the effectiveness of drug therapy in inhibiting viral production and preventing new infections. Furthermore, the model undergoes qualitative analysis, and we provide numerical simulations to illustrate our theoretical results.

2020 Mathematics Subject Classification. 34D20, 37M05, 37N25, 92D30.

Key words and phrases. HIV infection; CTL response; therapy; stability analysis.

1. Introduction

The human immunodeficiency virus (HIV) is a type of lentivirus, which belongs to the retrovirus subgroup. This virus damages immune system cells, ultimately leading to the well-known condition known as acquired immunodeficiency syndrome (AIDS) (see [1,2]). Presently, there is neither a cure nor a vaccine for HIV [3]. Nevertheless, antiretroviral therapy (ART) is employed for managing HIV infections. Two main categories of antiretroviral medications are approved for treating individuals infected with HIV: reverse transcriptase inhibitors (RTIs) and protease inhibitors (PIs) [4]. RTIs function by inhibiting the conversion of the virus's RNA into DNA during reverse transcription. This action helps keep the viral population in check and maintains a higher count of CD4+ T cells. On the other hand, PIs work by blocking the production of viruses within actively infected CD4+ T cells.

Over the past few decades, numerous mathematical models have been formulated to comprehensively

DOI: 10.28924/APJM/10-49

describe, comprehend, and manage the dynamics of HIV infection, for example in [5–13] and the references therein. More recently, an adapted model that accounts for two saturated rates, CTL response and therapy has been presented in a study by Lahm et al. [14]:

$$\begin{cases} \dot{x}(t) = \lambda - d\,x(t) - \big(1-u_1(t)\big)\dfrac{\beta\, v_I\, x}{1+a\, v_I} + r\, y, \\ \dot{y}(t) = \big(1-u_1(t)\big)\dfrac{\beta\, v_I\, x}{1+a\, v_I} - \big(\delta + r\big)y - pyz, \\ \dot{v}_I(t) = \big(1-u_2(t)\big)ky - \mu\, v_I, \\ \dot{v}_{NI}(t) = u_2(t)\, k\, y - \mu\, v_{NI}, \\ \dot{z}(t) = \dfrac{c\, y\, z}{1+\alpha\, y} - b\, z \end{cases} \tag{1}$$

In this proposed model, the variables x, y, v_I,v_{NI} and z correspond to distinct concentrations: uninfected cells, infected cells, free virus unaffected by protease inhibitors (PIs), free virus influenced by PIs, and cytotoxic T lymphocyte (CTL) cells, respectively. The population of susceptible host cells, $CD4^+$ T cells, is generated at a rate λ, experiences natural death at a rate dx, and becomes infected by the virus at a rate $\dfrac{(1-u_1(t))\beta v_I x}{1+ax}$. The parameter ry characterizes the rate at which infected cells are reverted to susceptible host cells due to noncytolytic processes (for more details see [15,16]). Infected cells are eliminated at a rate δy and are targeted by the CTL response at a rate pyz. Free virus not influenced by PIs is produced by infected cells at a rate $(1-u_2(t))ky$, while free virus influenced by PIs is generated by infected cells at a rate $u_2(t)ky$. CTLs proliferate in response to viral antigens derived from infected cells at a rate $\dfrac{cyz}{1+\alpha y}$ and undergo decay in the absence of antigenic stimulation at a rate bz. The control vector $u = (u_1(t), u_2(t))$ represents time-dependent antiviral therapy. The first component $u_1(t)$ signifies the efficacy of drug therapy in impeding new infections, whereas the second component $u_2(t)$ denotes the efficacy of drug therapy in suppressing viral production.

The model incorporates two key saturated rates, denoted as "a" and "α". These rates serve distinct purposes: "a" captures the saturated mass action linked to viral infection rates, with its behavior being well-documented by sources such as [17,18]. On the other hand, "α" represents a saturated function that characterizes the proliferation of cytotoxic T lymphocytes (CTLs). This proliferation is tempered by the influence of immune impairment caused by HIV infection, a phenomenon discussed in [19]. In the context of this paper, we adopt a simplification by treating the two considered treatments as constants. Consequently, the dynamic variables, previously represented by functions "$u_1(t)$" and "$u_2(t)$", are now approximated by the constants "η" a and "ϵ", respectively. As a result, the mathematical representation of the model, initially expressed by equation (1), can be redefined as follows:

$$\begin{cases} \dot{x}(t) = \lambda - d\,x(t) - \big(1-\eta\big)\dfrac{\beta\, v_I\, x}{1+a\, v_I} + r\, y, \\ \dot{y}(t) = \big(1-\eta\big)\dfrac{\beta\, v_I\, x}{1+a\, v_I} - \big(\delta + r\big)y - pyz, \\ \dot{v}_I(t) = \big(1-\epsilon\big)ky - \mu\, v_I, \\ \dot{v}_{NI}(t) = \epsilon\, k\, y - \mu\, v_{NI}, \\ \dot{z}(t) = \dfrac{c\, y\, z}{1+\alpha\, y} - b\, z \end{cases} \tag{2}$$

The objective of this study is to analyze the dynamic characteristics of the newly modified model. To achieve this, the remainder of the paper is structured as follows: Section 2, is dedicated to exploring the positivity and boundedness of solutions within the context of the model. In Section 3, a detailed analysis of the new described model. Results obtained by numerical simulations are given in Section 4 and we conclude in the last section.

2. Positivity and Boundedness of Solutions

In this section, our focus is directed towards substantiating two fundamental aspects concerning the solutions within the framework of system (2). Given that this system governs the dynamics of a cell population, it is imperative to establish both the positivity and boundedness of the solutions. These attributes hold paramount importance as they ensure that the cell densities, integral to the system, remain not only non-negative but also confined within reasonable limits. By attaining these crucial properties, we lay the groundwork for asserting the global existence of solutions. This, in turn, underscores the model's capacity to sustain its solutions over extended temporal domains, thus reinforcing the credibility and applicability of our cell population evolution depiction. To this end and for biological reasons, we assume that the initial data for system (2) satisfy:

$$x_0 \geq 0,\ y_0 \geq 0,\ V_{I_0} \geq 0 \text{ and } V_{NI_0} \geq 0.$$

Hence, we have the following result:

Proposition 2.1. *For any initial conditions* $(x_0,\ y_0,\ V_{I_0},\ V_{NI_0})$*, system* (2) *has a unique solution. Moreover, this solution is nonnegative and bounded for all* $t > 0$*. Additionally, if we note*

$$x_1(t) = x(t) + y(t) \text{ and } \delta_1 = \min(d; \delta),$$

Then, we have:

i) $x_1(t) \leq x_1(0) + \dfrac{\lambda}{\delta_1}$,

ii) $v_I(t) \leq v_I(0) + \dfrac{\big(1-\varepsilon\big)\, k}{\mu}\|y\|_\infty$,

iii) $v_{NI}(t) \leq v_{NI}(0) + \dfrac{\varepsilon\, k}{\mu}\|y\|_\infty$,

iv) $z(t) \leq z(0) + \frac{c}{p}\big[\max(1; 2 - \frac{d}{b})\, x(0) + y(0) + \max(\frac{\lambda}{b}; \frac{\lambda}{d}) + \max(0; 1 - \frac{\delta}{b})\, |y\|_\infty\big]$.

Proof. By the classical proposition [20, A.1], we can confirm that the unique solution,

$$(x(t), y(t), v_I(t), v_{NI}(t), z(t)) \in \mathbb{R}^5_+.$$

Move now to prove (i). To this end, we add the first and second equation in (2), to get

$$\dot{x_1} = \lambda - dx - \delta y - pyz,$$

then,

$$x_1(t) \leq x_1(0)e^{-\delta_1 t} + \frac{\lambda}{\delta_1}(1 - e^{-\delta_1 t}) \quad \text{where} \quad \delta_1 = \min(d; \delta).$$

Using the fact that $0 \leq e^{-\delta_1 t} \leq 1$, we deduce (i).

Next, from the equation $\dot{v_I} = (1-\epsilon)ky - \mu v_I$, we obtain

$$v_I(t) = v_I(0)e^{-\mu t} + (1-\epsilon)k \int_0^t y(\xi)e^{(\xi - t)\mu} d\xi,$$

then,

$$v_I(t) \leq v_I(0) + \frac{(1-\epsilon)k}{\mu} \|y\|_\infty (1 - e^{-\mu t})$$

Since $1 - e^{-\mu t} \leq 1$, we get (ii).

Now, the equation $\dot{v}_{NI} = \epsilon ky - \mu v_{NI}$ implies

$$v_{NI}(t) = v_{NI}(0)e^{-\mu t} + \epsilon k \int_0^t y(\xi)e^{(\xi - t)\mu} d\xi$$

then,

$$v_{NI}(t) \leq v_{NI}(0) + \frac{\epsilon k}{\mu} \|y\|_\infty (1 - e^{-\mu t})$$

Note that $0 \leq 1 - e^{-\mu t} \leq 1$. Them, we can now deduce (iii).

Finally, from the equation $\dot{z} = \dfrac{cyz}{1 + \alpha y} - bz$ implies

$$\dot{z} + bz \leq cyz.$$

Since $cyz = \frac{c}{p}[\lambda - (\dot{x} + dx) - (\dot{y} + \delta y)]$, we have

$$\begin{aligned} z(t) \leq [\frac{c}{p}(x(0) + y(0) - \frac{\lambda}{b}) + z(0)]e^{-bt} \\ + \frac{c}{p}\{\frac{\lambda}{b} + \int_0^t [(b-d)T(\xi) + (b-\delta)y(\xi)]e^{b(\xi - t)} d\xi - x(t) - y(t)\}. \end{aligned}$$

Then,

Case 1: If $b-d \leq 0$ et $b-\delta \leq 0$, we have

$$z(t) \leq z(0) + \frac{c}{p}\Big[\frac{\lambda}{b} + x(0) + y(0)\Big].$$

Case 2: If $b-d \leq 0$ et $b-\delta \geq 0$, we have

$$z(t) \leq z(0) + \frac{c}{p}\Big[\frac{\lambda}{b} + x(0) + y(0) + (1-\frac{\delta}{b})\|y\|_\infty\Big].$$

Case 3: If $b-d \geq 0$ et $b-\delta \leq 0$, we have

$$z(t) \leq z(0) + \frac{c}{p}\Big[\frac{\lambda}{d} + \Big(2-\frac{d}{b}\Big)x(0) + y(0)\Big].$$

Case 4: If $b-d \geq 0$ et $b-\delta \geq 0$, we have

$$z(t) \leq z(0) + \frac{c}{p}\Big[\frac{\lambda}{d} + \Big(2-\frac{d}{b}\Big)x(0) + y(0) + (1-\frac{\delta}{b})\|y\|_\infty\Big].$$

Therfore, we have proved that all the cases imply (iv). □

3. Stability Analysis of the Model

This section is dedicated to conducting a stability analysis of both the disease-free equilibrium and the endemic equilibrium points. Additionally, numerical simulations will be provided for each specific case.

3.1. **Stability of the disease-free equilibrium.** System (2) has an infection-free equilibrium $E_f = (\frac{\lambda}{d}, 0, 0, 0, 0)$, corresponding to the maximal level of healthy CD4$^+$ T-cells. By a simple calculation, the basic reproduction number of (2) is given by

$$R_0 = \frac{(1-\theta)\beta k\lambda}{d\mu(\delta+r)}. \tag{3}$$

Here, we put $\theta = \eta + \epsilon - \eta\epsilon$, which represents the combined efficacy of the two drugs. Then $1-\theta = (1-\eta)(1-\epsilon)$ which implies that each drug acts independently. At any arbitrary point, the Jacobian matrix of the system (2), is given by

$$J = \begin{pmatrix} -d - \frac{(1-\eta)\beta v_I}{1+av_I} & r & -\frac{(1-\eta)\beta x}{(1+av_I)^2} & 0 & 0 \\ \frac{(1-\eta)\beta v_I}{1+av_I} & -(\delta+r)-pz & \frac{(1-\eta)\beta x}{(1+av_I)^2} & 0 & -py \\ 0 & (1-\epsilon)k & -\mu & 0 & 0 \\ 0 & \epsilon k & 0 & -\mu & 0 \\ 0 & \frac{cz}{(1+\alpha y)^2} & 0 & 0 & \frac{cy}{1+\alpha y} - b \end{pmatrix} \tag{4}$$

Then, we have the following result,

Theorem 3.1. *The disease-free equilibrium, E_f, is locally asymptotically stable for $R_0 < 1$.*

Proof. At the disease-free equilibrium point, E_f, we can characterize the Jacobian matrix as follows:

$$J_{E_f} = \begin{pmatrix} -d & r & -\frac{(1-\eta)\beta\lambda}{d} & 0 & 0 \\ 0 & -(\delta+r) & \frac{(1-\eta)\beta\lambda}{d} & 0 & 0 \\ 0 & (1-\epsilon)k & -\mu & 0 & 0 \\ 0 & \epsilon k & 0 & -\mu & 0 \\ 0 & 0 & 0 & 0 & -b \end{pmatrix}. \tag{5}$$

The characteristic polynomial of J_{E_f} is

$$P_{E_f}(\xi) = (\xi+d)(\xi+b)(\xi+\mu)[\xi^2 + (\delta+r+\mu)\xi + (\delta+r)\mu(1-R_0)],$$

then the eigenvalues of the matrix J_{E_f} are

$$\xi_1 = -d,$$

$$\xi_2 = -b,$$

$$\xi_3 = -\mu,$$

$$\xi_4 = \frac{-(\delta+r+\mu) - \sqrt{(\delta+r+\mu)^2 - 4(\delta+r)\mu(1-R_0)}}{2},$$

$$\xi_5 = \frac{-(\delta+r+\mu) + \sqrt{(\delta+r+\mu)^2 - 4(\delta+r)\mu(1-R_0)}}{2}.$$

It is evident that ξ_1, ξ_2, ξ_3 and ξ_4 are negative Furthermore, when $R_0 < 1$, ξ_5 also becomes negative, implying that E_f is locally asymptotically stable. □

To confirm the above theoretical result, we give the following numerical result.

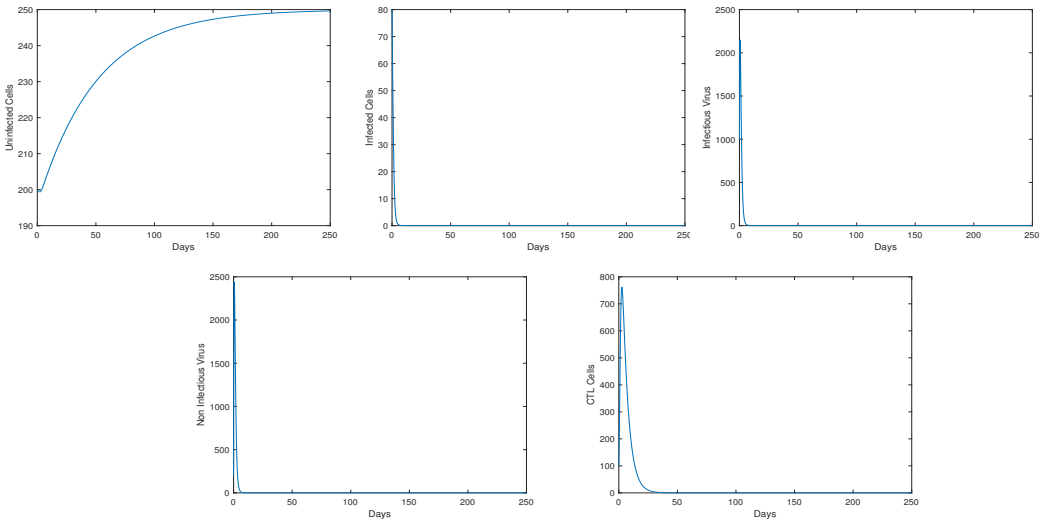

FIGURE 1. Behavior of the infection during the time for $\lambda = 5$, $\beta = 0.000024$, $d = 0.02$, $\delta = 0.5$, $p = 0.001$, $k = 250$, $\mu = 3$, $r = 0.01$, $a = 0.001$, $\alpha = 0.001$, $c = 0.03$, $b = 0.2$, $\eta = 0.4$ and $\epsilon = 0.55$, which pertain to the stability of the free equilibrium E_f.

3.2. **Infection steady states.** In this section, we focus on the existence and stability of the infection's steady state. Indeed, it is easily verified that the system (2) encompasses two such states:

$$E_1 = (x_1, y_1, v_{I_1}, v_{NI_1}, 0) \qquad \text{and} \qquad E_2 = (x_2, y_2, v_{I_2}, v_{NI_2}, z_2),$$

where

$$x_1 = \frac{\lambda(\mu\delta + a(1-\epsilon)k\lambda)}{d(\mu\delta R_0 + a(1-\epsilon)k\lambda)}, \qquad y_1 = \frac{\lambda\mu(R_0-1)}{(\mu\delta R_0 + a(1-\epsilon)k\lambda)},$$
$$v_{I_1} = \frac{(1-\epsilon)k}{\mu}.y_1, \qquad v_{NI_1} = \frac{\epsilon k}{\mu}\, y_1,$$

and

$$x_2 = \frac{(a(1-\epsilon)kr)y_2^2 + (a(1-\epsilon)k\lambda + \mu r)y_2 + \mu\lambda}{(1-\epsilon)k(ad + (1-\eta)\beta)y_2 + \mu d}, \qquad y_2 = \frac{b}{c - \alpha b}$$
$$v_{I_2} = \frac{(1-\epsilon)ky_2}{\mu}, \qquad v_{NI_2} = \frac{\epsilon k y_2}{\mu},$$
$$z_2 = \frac{-(1-\epsilon)k[adr + \delta(ad + (1-\eta)\beta)]y_2 + ((1-\theta)\beta k\lambda - d\mu(r+\delta))}{p((1-\epsilon)k(ad + (1-\eta)\beta)y_2 + \mu d)}.$$

In order to study the local stability of the points E_1 and E_2, we first define the following numbers:

$$D_0 = \frac{c\lambda}{b\delta}, \; H_0 = \frac{1}{\frac{1}{R_0} + \frac{1}{\widetilde{D_0}}}$$
$$\widetilde{D_0} = D_0 \frac{\mu\delta R_0}{a(1-\epsilon)k\lambda + \mu\delta R_0 + \alpha\mu\lambda(R_0-1)},$$

We begin with the following result concerning the first point E_1,

Theorem 3.2. *We have the following cases,*

(1) *If $R_0 < 1$, then the point E_1 does not exist.*
(2) *If $R_0 = 1$, then $E_1 = E_f$.*
(3) *If $R_0 > 1$ and $H_0 < 1$ then E_1 is locally asymptotically stable.*
(4) *If $R_0 > 1$ and $H_0 > 1$ then E_1 is unstable.*

Proof. It is easy to observe that if $R_0 < 1$, then the point E_1 does not exist. Additionally, when $R_0 = 1$, the two points E_1 and E_f coincide. In the case of $R_0 > 1$, the Jacobian matrix at E_1 is given by:

$$J_{E_1} = \begin{pmatrix} -d - \frac{(1-\eta)\beta v_{I_1}}{1+av_{I_1}} & r & -\frac{(1-\eta)\beta x_1}{(1+av_{I_1})^2} & 0 & 0 \\ \frac{(1-\eta)\beta v_{I_1}}{1+av_{I_1}} & -(\delta+r) & \frac{(1-\eta)\beta x_1}{(1+av_{I_1})^2} & 0 & -py_1 \\ 0 & (1-\epsilon)k & -\mu & 0 & 0 \\ 0 & \epsilon k & 0 & -\mu & 0 \\ 0 & 0 & 0 & 0 & \frac{cy_1}{1+\alpha y_1} - b \end{pmatrix}.$$

Then, its characteristic equation is

$$(\xi+\mu)(\xi+b-\frac{cv_{I_1}}{1+\alpha v_{I_1}})(\xi^3+a_1\xi^2+a_2\xi+a_3)=0,$$

where

$$\begin{aligned}
a_1 &= d+\delta+\mu+r+\frac{(1-\eta)\beta v_{I_1}}{1+av_{I_1}},\\
a_2 &= (\delta+\mu+r)d+(\mu+\delta)\frac{(1-\eta)\beta v_{I_1}}{1+av_{I_1}}\\
&\qquad +\mu(\delta+r)-\frac{(1-\theta)N\delta\beta x_1}{(1+av_{I_1})^2},\\
a_3 &= \mu d(\delta+r)+\frac{\mu\delta(1-\eta)\beta v_{I_1}}{1+av_{I_1}}-\frac{(1-\theta)N\delta\beta x_1 d}{(1+av_{I_1})^2}.
\end{aligned}$$

We have $\xi_1=-\mu<0$ and $\xi_2=\dfrac{cv_{I_1}}{1+\alpha v_{I_1}}-b=\dfrac{b\widetilde{D_0}(H_0-1)}{H_0}$ as the two eigenvalues of J_{E_1}. The sign of the eigenvalue ξ_1 is negative when $H_0<1$, zero when $H_0=1$, and positive when $H_0>1$. Moreover, since $R_0>1$, we have $a_1>0$ and $a_1\,a_2-a_3>0$. According to the Routh-Hurwitz Theorem [21], the remaining eigenvalues of J_{E_1} have negative real parts. Therefore, E_1 is unstable when $H_0>1$ and locally asymptotically stable when $R_0>1$ and $H_0<1$. □

To validate the aforementioned theoretical result, we present the following numerical result,

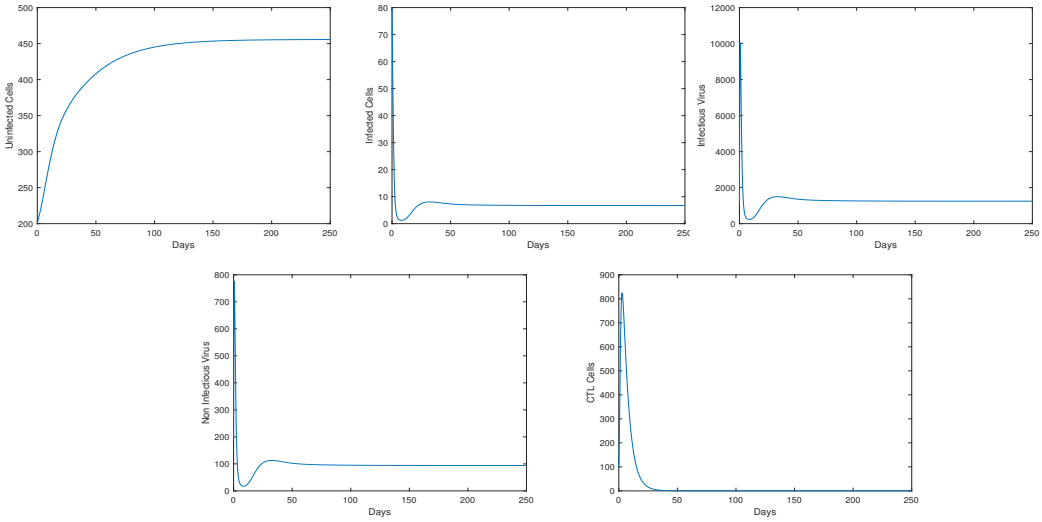

FIGURE 2. Behavior of the infection during the time for $\lambda=5$, $\beta=0.000024$, $d=0.02$, $\delta=0.5$, $p=0.001$, $k=600$, $\mu=3$, $r=0.01$, $a=0.001$, $\alpha=0.001$, $c=0.03$, $b=0.2$, $\eta=0.1$ and $\epsilon=0.2$, which correspond to the stability of the endemic-equilibrium point E_1.

Now, let's proceed to the second point, E_2, to demonstrate the following result,

Theorem 3.3. *We have the following cases,*

(1) *If* $\alpha > \frac{c}{b}$ *or* $H_0 < 1$, *then the point* E_2 *does not exist and* $E_2 = E_1$ *when* $H_0 = 1$.

(2) *If* $\alpha < \frac{c}{b}$ *and* $H_0 > 1$, *then* E_2 *is locally asymptotically stable.*

Proof. We notice that the condition $\alpha < \frac{c}{b}$ and $H_0 > 1$ is equivalent to $y_2 < y_1$. It easy to verify that the point E_2 does not exists if $H_0 < 1$ or $\alpha > \frac{c}{b}$. Moreover, we have $E_2 = E_1$ for $H_0 = 1$. We assume now that $\alpha < \frac{c}{b}$ and $H_0 > 1$; the Jacobian matrix at E_2 is

$$J_{E_2} = \begin{pmatrix} -d - \frac{(1-\eta)\beta v_{I_2}}{1+av_{I_2}} & r & -\frac{(1-\eta)\beta x_2}{(1+av_{I_2})^2} & 0 & 0 \\ \frac{(1-\eta)\beta v_{I_2}}{1+av_{I_2}} & -(\delta+r)-pz_2 & \frac{(1-\eta)\beta x_2}{(1+av_{I_2})^2} & 0 & -py_2 \\ 0 & (1-\epsilon)k & -\mu & 0 & 0 \\ 0 & \epsilon k & 0 & -\mu & 0 \\ 0 & \frac{cz_2}{(1+\alpha y_2)^2} & 0 & 0 & 0 \end{pmatrix}$$

The characteristic equation associated with J_{E_2} is given by,

$$(\xi+\mu)(\xi^4 + c_1\xi^3 + c_2\xi^2 + c_3\xi + c_4) = 0 \tag{6}$$

where

$$\begin{aligned} c_1 &= B_1 + d + r + \delta + \mu + pz_2, \\ c_2 &= pz_2(B_1 + cB_3y_2 + d + \mu) + d\mu + dr + d\delta \\ &\qquad + \mu r + \mu B_1 + \mu\delta + B_1\delta + (1-\epsilon)kB_2, \\ c_3 &= cB_3py_2z_2(d + \mu + B_1) + \mu pz_2(d + B_1) \\ &\qquad + d\mu r + d\mu\delta + \mu B_1\delta + +dk(1-\epsilon)B_2, \\ c_4 &= cz_2B_3py_2\mu(d + B_1). \end{aligned}$$

where

$$B_1 = \frac{(1-\eta)\beta v_{I_2}}{1+av_{I_2}},\ B_2 = \frac{(1-\eta)\beta x_2}{(1+av_{I_2})^2},\ B_3 = (1+\alpha y_2)^{-2}.$$

We note that $\xi_1 = -\mu < 0$ an eigenvalue of J_{E_2}. Moreover, $c_1 > 0$ and $c_1c_2 - c_3 > 0$. Then, The Routh-Hurwitz Theorem found in [21], implies that the other eigenvalues of J_{E_2} have negative real parts. Consequently, E_2 is unstable when $H_0 < 1$, locally asymptotically stable when $H_0 > 1$. □

The numerical result in Figure 3, confirms the above theoretical result.

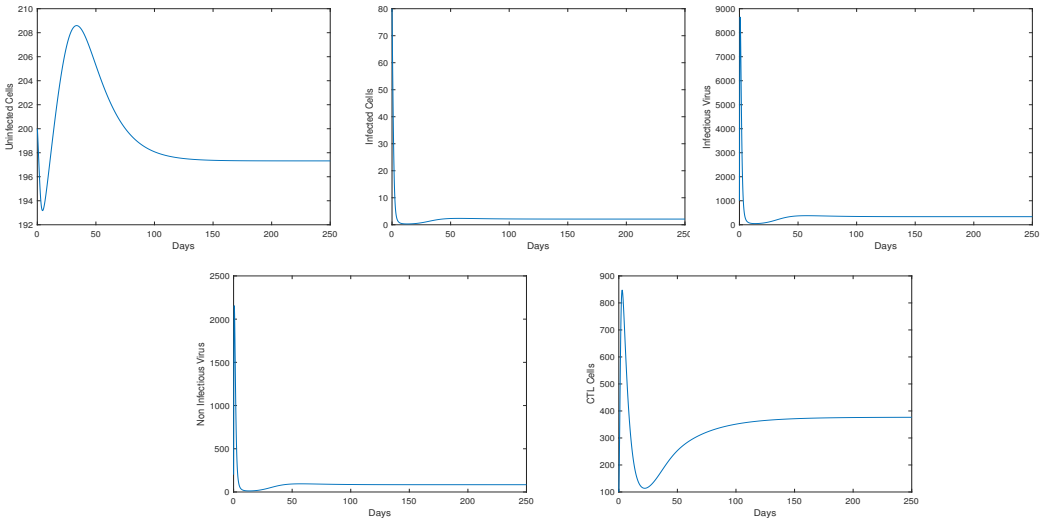

FIGURE 3. Behavior of the infection during the time for $\lambda = 15$, $\beta = 0.000024$, $d = 0.02$, $\delta = 0.5$, $p = 0.001$, $k = 600$, $\mu = 3$, $r = 0.01$, $a = 0.001$, $\alpha = 0.001$, $c = 0.03$, $b = 0.2$, $\eta = 0.02$ and $\epsilon = 0.07$, which correspond to the stability of the endemic-equilibrium point E_2.

4. Numerical simulations

For our numerical simulations, we employed the Euler finite-difference scheme method to discretize the system of five equations. The simulation parameters were inspired by references [12,13,22,23]. We also incorporated initial conditions that align with clinical data for HIV-infected individuals during the symptomatic phase [24].

In Figure 1, we present the infection's evolution during the first 250 days for the free-equilibrium case. Figure 2 illustrates a scenario where $R_0 > 1$ and $H_0 < 1$, resulting in a rapid decline in CTL cells and persistent infection over time. A straightforward calculation reveals that when $R_0 > 1$, the condition for the local asymptotic stability of E_1 is equivalent to:

$$D_0 < (\frac{R_0}{R_0 - 1}) \frac{a(1-\epsilon)k\lambda + \mu\delta R_0 + \alpha\mu\lambda(R_0 - 1)}{\mu\delta R_0},$$

this condition indicates that if D_0 falls below the threshold mentioned above, the immune response cannot keep pace with the infection, leading to its eventual disappearance.

Figure 3 depicts a scenario where $\alpha < \frac{c}{b}$ and $H_0 > 1$, resulting in an increase in CD4$^+$ cell count and a slight reduction in virus load. 4 Through a simple calculation, we establish that under the condition $\alpha < \frac{c}{b}$, the local asymptotic stability of E_2 is equivalent to:

$$D_0 > (\frac{R_0}{R_0 - 1}) \frac{a(1-\epsilon)k\lambda + \mu\delta R_0 + \alpha\mu\lambda(R_0 - 1)}{\mu\delta R_0},$$

this condition signifies that if D_0 surpasses the threshold mentioned, the immune response, particularly CTL, can effectively reduce the virus concentration.

5. Conclusion

In this study, we have delved into the dynamics of Human Immunodeficiency Virus (HIV) during therapy and the activation of cytotoxic T-lymphocytes (CTL) cells. Our model incorporates two saturated rates to provide a more accurate representation of viral infection and CTL proliferation. We have rigorously demonstrated the positivity and boundedness of solutions, and we have thoroughly examined the stability of both disease-free equilibrium and endemic equilibria.

The disease-free steady state exhibits local asymptotic stability when the basic reproduction number (R_0) is less than unity $(R_0 < 1)$. When $R_0 > 1$, we establish the existence of two infection steady states. The local stability of these infection steady states depends on both the basic reproduction number R_0 and the CTL immune response reproduction number D_0.

Interestingly, the formula for R_0 reveals that it is independent of the parameters governing CTL activation (b, c, α, and p). This suggests that CTL alone may not eliminate the virus entirely. However, they can effectively reduce the viral load concentration and increase the concentration of healthy $CD4^+$ cells. This becomes evident when comparing the components of viral load and those of $CD4^+$ concentration before and after CTL activation, especially under the condition $H_0 > 1$.

In fact, simple calculations demonstrate that $x_1 < x_2$ and $V_{I_2} < V_{I_1}$, where x_1, x_2, V_{I_1}, and V_{I_2} are defined above. These findings indicate that the cellular immune response can effectively control the virus load.

References

[1] R.A. Weiss, How does HIV cause AIDS?, Science. 260 (1993), 1273–1279. https://doi.org/10.1126/science.8493571.

[2] W. Blattner, R.C. Gallo, H.M. Temin, HIV causes AIDS, Science. 241 (1988), 515–515. https://doi.org/10.1126/science.3399881.

[3] C.J. Silva, D.F.M. Torres, A TB-HIV/AIDS coinfection model and optimal control treatment, Discr. Contin. Dyn. Syst. - A. 35 (2015), 4639–4663. https://doi.org/10.3934/dcds.2015.35.4639.

[4] Panel on Antiretroviral Guidelines for Adults and Adolescents, Guidelines for the use of antiretroviral agents in HIV-1-infected adults and adolescents, Department of Health and Human Services, 1–167, (2011).

[5] N. Bairagi, D. Adak, Global analysis of HIV-1 dynamics with Hill type infection rate and intracellular delay, Appl. Math. Model. 38 (2014), 5047–5066. https://doi.org/10.1016/j.apm.2014.03.010.

[6] K. Allali, Y. Tabit, S. Harroudi, On HIV model with adaptive immune response, two saturated rates and therapy, Math. Model. Nat. Phenom. 12 (2017), 1–14. https://doi.org/10.1051/mmnp/201712501.

[7] B. EL Boukari, K. Hattaf, N. Yousfi, Modeling the therapy of HIV infection with CTL response and cure rate, Int. J. Ecol. Econ. Stat. 28 (2013), 1–17.

[8] S. Harroudi, D. Bentaleb, Y. Tabit, S. Amine, K. Allali, Optimal control of an HIV infection model with the adaptive immune response and two saturated rates, Int. J. Math. Comp. Sci. 14 (2019), 787–807.

[9] K. Hattaf, N. Yousfi, Optimal control of a delayed HIV infection model with immune response using an efficient numerical method, ISRN Biomath. 2012 (2012), 215124. https://doi.org/10.5402/2012/215124.

[10] M.A. Nowak, R.M. May, Mathematical biology of HIV infections: antigenic variation and diversity threshold, Math. Biosci. 106 (1991), 1–21. https://doi.org/10.1016/0025-5564(91)90037-j.

[11] A.S. Perelson, P.W. Nelson, Mathematical analysis of HIV-1 dynamics in vivo, SIAM Rev. 41 (1999), 3–44. https://doi.org/10.1137/s0036144598335107.

[12] Y. Tabit, K. Hattaf, N. Yousfi, Dynamics of an HIV pathogenesis model with CTL immune response and two saturated rates, World J. Model. Simul. 10 (2014), 215–223.

[13] Y. Tabit, A. Meskaf, K. Allali, Mathematical analysis of HIV model with two saturated rates, CTL and antibody responses, World J. Model. Simul. 12 (2016), 137–146.

[14] B. Lahmidani, O. Baiz, Y. Tabit, D. El Moutawakil, Optimal control of an HIV infection model with the CTL response and two saturated rates, Int. J. Appl. Math. 34 (2021), 1093–1109. https://doi.org/10.12732/ijam.v34i6.4.

[15] X. Zhou, X. Song, X. Shi, A differential equation model of HIV infection of CD4+ T-cells with cure rate, J. Math. Anal. Appl. 342 (2008), 1342–1355. https://doi.org/10.1016/j.jmaa.2008.01.008.

[16] X. Liu, H. Wang, Z. Hu, W. Ma, Global stability of an HIV pathogenesis model with cure rate, Nonlinear Anal.: Real World Appl. 12 (2011), 2947–2961. https://doi.org/10.1016/j.nonrwa.2011.04.016.

[17] X. Song, A.U. Neumann, Global stability and periodic solution of the viral dynamics, J. Math. Anal. Appl. 329 (2007), 281–297. https://doi.org/10.1016/j.jmaa.2006.06.064.

[18] Q. Sun, L. Min, Dynamics analysis and simulation of a modified HIV infection model with a saturated infection rate, Comp. Math. Meth. Med. 2014 (2014), 145162. https://doi.org/10.1155/2014/145162.

[19] S. Iwami, T. Miura, S. Nakaoka, Y. Takeuchi, Immune impairment in HIV infection: Existence of risky and immunodeficiency thresholds, J. Theor. Biol. 260 (2009), 490–501. https://doi.org/10.1016/j.jtbi.2009.06.023.

[20] H.R. Thieme, Mathematics in population biology, Princeton University Press, Princeton, (2003).

[21] I.S. Gradshteyn, I.M. Ryzhik, Routh Hurwitz theorem, 6th ed. in: Tables of Integrals, Series, and Products, Academic Press, San Diego, CA, 2000.

[22] R. Fister, S. Lenhart, J. S. McNally, Optimizing chemotherapy in an HIV model, Elec. J. Diff. Equ. 1998 (1998), 32, pp. 1–12.

[23] S. Butler, D. Kirschner, S. Lenhart, Optimal control of chemotherapy affecting the infectivity of HIV. In: O. Arino, D. Axelrod, M. Kimmel, M. Langlais, (eds.) Advances in Mathematical Population Dynamics: Molecules, Cells, Man, pp. 104–120. World Scientific Publishing, (1997).

[24] K. Hattaf, N. Yousfi, Two optimal treatments of HIV infection model, World J. Model. Simul. 8 (2012), 27–35.